

Kinetics and Mechanism of Iridium-Catalyzed Dehydrogenation of Primary Amines to Nitriles

Wesley H. Bernskoetter and Maurice Brookhart*

Department of Chemistry, The University of North Carolina at Chapel Hill,
Chapel Hill, North Carolina 27599-3290

Received November 14, 2007

A family of primary amines has been catalytically dehydrogenated to nitriles by $[\text{C}_6\text{H}_3\text{-2,6-(OP}^t\text{Bu}_2)_2]\text{IrH}_2$ using *tert*-butylethylene as a hydrogen acceptor. The catalytic mechanism has been investigated by a series of kinetic and isotopic labeling experiments, in addition to the isolation of intermediates along the reaction pathway. The turnover frequency exhibits a first-order dependence on the concentration of amine, an inverse first-order dependence on nitrile, and a zero-order dependence on *tert*-butylethylene. The mechanism of amine dehydrogenation is proposed to proceed from an iridium(I) nitrile complex, the catalyst resting state, via two preturnover limiting equilibria, followed by a slow β -hydride elimination event from a transient iridium(III) amido hydride species. Measuring rate constants for the stoichiometric dehydrogenation of isobutylamine over a 41 °C temperature range established activation parameters for β -hydride elimination of ΔH^\ddagger 24.8(9) kcal/mol and $\Delta S^\ddagger = -10(2)$ eu. Dehydrogenation of a series of *para*-substituted benzyl amines indicated enhanced conversions to nitriles for substrates bearing electron-donating substituents.

Introduction

Transition metal-mediated amine oxidation offers an attractive route to important organic synthons such as enamines, imines, and nitriles.¹ Recently iridium “pincer” complexes² have shown promise for amine dehydrogenations; in particular $[\text{C}_6\text{H}_3\text{-2,6-(CH}_2\text{P}^t\text{Bu}_2)_2]\text{IrH}_2$ has proven competent for the catalytic formation of imines³ and enamines⁴ from secondary and tertiary amines, respectively. Goldman and co-workers have also observed the stoichiometric iridium-mediated dehydrogenation of secondary amines coupled with C–C bond cleavage to afford iridium(III) isocyanide species.⁵ However, the catalytic synthesis of nitriles, the most oxidized amine dehydrogenation product, has yet to be explored with this class of robust iridium compounds.

Currently numerous methods exist for the stoichiometric and catalytic oxidation of amines to nitriles; however these procedures often employ harsh oxidants and generate hazardous byproducts.⁶ The most effective transition metal-mediated versions of this reaction also utilize strong inorganic oxidants.⁷ Yamazaki and co-workers have reported that nickel(II) sulfate successfully dehydrogenates a variety of primary amines to nitriles in an aqueous base solution with an excess of potassium peroxydisulfate.⁸ Significantly, this reagent mixture achieves high isolated yields of nitriles (>90%) at ambient temperature with nickel loadings of ≤ 2 mol %. More recently related ruthenium-catalyzed amine dehydrogenation reactions have also been developed with $\text{RuCl}_3 \cdot n\text{H}_2\text{O}/\text{K}_2\text{S}_2\text{O}_8/\text{KOH}$, which offer activities comparable to nickel(II) sulfate.⁹ The mechanisms and catalytically active species in these amine oxidation procedures have not been fully elucidated.

An alternative to the use of strong oxidants for amine dehydrogenation is to employ a simple olefin as the hydrogen acceptor. This procedure offers a mechanistically distinct and relatively benign pathway for nitrile synthesis. Recently our laboratory has developed a series of iridium catalysts that are highly active for the transfer dehydrogenation of alkanes using *tert*-butylethylene as the oxidizing agent (Figure 1).¹⁰ Herein we describe the application of a related iridium pincer complex as a precatalyst for the transfer dehydrogenation of primary amines to nitriles. The mechanism of amine oxidation has been

* Corresponding author. E-mail: mbrookhart@unc.edu.

(1) Murahashi, S.; Imada, Y. Amine Oxidation. In *Transition Metals for Organic Synthesis*, 2nd ed.; Wiley-VCH: Weinheim, 2004; pp 497–507.

(2) (a) Renkema, K. B.; Kissin, Y. V.; Goldman, A. S. *J. Am. Chem. Soc.* **2003**, *125*, 7770. (b) Krogh-Jespersen, K.; Czerw, M.; Summa, N.; Renkema, K. B.; Achord, P. D.; Goldman, A. S. *J. Am. Chem. Soc.* **2002**, *124*, 11404. (c) Krogh-Jespersen, K.; Czerw, M.; Zhu, K.; Singh, B.; Kanzelberger, M.; Darji, N.; Achord, P. D.; Renkema, K. B.; Goldman, A. S. *J. Am. Chem. Soc.* **2002**, *124*, 10797. (d) Li, S.; Hall, M. B. *Organometallics* **2001**, *20*, 2153. (e) Morales-Morales, D.; Lee, D. W.; Wang, Z.; Jensen, C. M. *Organometallics* **2001**, *20*, 1144. (f) Krogh-Jespersen, K.; Czerw, M.; Kanzelberger, M.; Goldman, A. S. *J. Chem. Inf. Comput. Sci.* **2001**, *41*, 56. (g) Kanzelberger, M.; Singh, B.; Czerw, M.; Krogh-Jespersen, K.; Goldman, A. S. *J. Am. Chem. Soc.* **2000**, *122*, 11017. (h) Liu, F.; Pak, E. B.; Singh, B.; Jensen, C. M.; Goldman, A. S. *J. Am. Chem. Soc.* **1999**, *121*, 4086. (i) Niu, S.; Hall, M. B. *J. Am. Chem. Soc.* **1999**, *121*, 3992. (j) Liu, F.; Goldman, A. S. *Chem. Commun.* **1999**, 655. (k) Lee, D. W.; Kaska, W. C.; Jensen, C. M. *Organometallics* **1998**, *17*, 1. (l) Gupta, M.; Hagen, C.; Kaska, C. W.; Cramer, R. E.; Jensen, C. M. *J. Am. Chem. Soc.* **1997**, *119*, 840. (m) Gupta, M.; Hagen, C.; Flesher, R. J.; Kaska, W. C.; Jensen, C. M. *Chem. Commun.* **1996**, 2083.

(3) Gu, X.; Chen, W.; Morales-Morales, D.; Jensen, C. M. *J. Mol. Catal. A* **2002**, *189*, 119.

(4) Zhang, X.; Fried, A.; Knapp, S.; Goldman, A. S. *Chem. Commun.* **2003**, 2060.

(5) Zhang, X.; Emge, T. J.; Ghosh, R.; Goldman, A. S. *J. Am. Chem. Soc.* **2005**, *127*, 8250.

(6) March, J. *Advanced Organic Chemistry: Reactions, Mechanisms, and Structure*, 2nd ed.; Wiley-Interscience, McGraw-Hill: New York, 1977; pp 1085–1086.

(7) (a) Aerobic oxidation of amines catalyzed by Ru complexes has also been reported, although with reduced selectivities: Bailey, A. J.; James, B. R. *Chem. Commun.* **1997**, 507. (b) Tang, R.; Diamond, S. E.; Neary, N.; Mares, F. *Chem. Commun.* **1978**, 562.

(8) Yamazaki, S.; Yamazaki, Y. *Bull. Chem. Soc. Jpn.* **1990**, *63*, 301.

(9) Griffith, W. P.; Reddy, B.; Shoaib, A. G. F.; Suriaatmaja, M.; White, A. J. P.; Williams, D. J. *Dalton Trans.* **1998**, 2819.

(10) Göttker-Schnetmann, I.; White, P.; Brookhart, M. J. *Am. Chem. Soc.* **2004**, *126*, 1804.

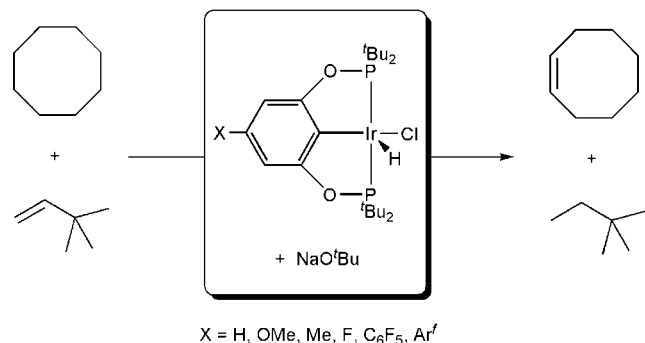
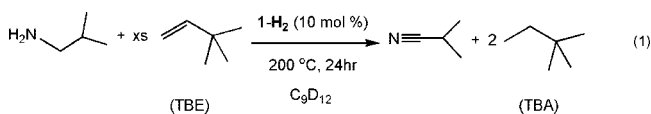


Figure 1. Highly active catalyst for alkane transfer dehydrogenation.

explored by kinetic and isotopic labeling studies and is supported by the dehydrogenation of a limited family of substrates.

Results and Discussion

Isobutylamine Dehydrogenation. The thermally robust pincer iridium complex $[\text{C}_6\text{H}_3\text{-}2,6\text{-(OP}^t\text{Bu}_2)_2\text{]IrH}_2$ (**1-H₂**)¹¹ has been implicated as a source of 14-electron iridium(I) in the presence of hydrogen acceptors.¹² This transiently generated species has shown some of the highest reported activities for homogeneous, thermal alkane transfer dehydrogenation.¹⁰ In light of this precedent, complex **1-H₂** was assayed as a precatalyst for amine dehydrogenation. A mestylene-*d*₁₂ solution of **1-H₂** was treated with 10 equiv of isobutylamine and 50 equiv of *tert*-butylethylene (TBE), then heated at 200 °C for 24 h (eq 1).¹³



Analysis by gas chromatography indicated >95% conversion to isobutyronitrile along with formation of 2,2-dimethylbutane (TBA).

Isolation of the organometallic reaction product following removal of all volatile materials afforded the iridium(I) nitrile adduct $[\text{C}_6\text{H}_3\text{-}2,6\text{-(OP}^t\text{Bu}_2)_2\text{]Ir(N}\equiv\text{C}^i\text{Pr)}$ (**1-NCⁱPr**). This orange crystalline solid was identified by independent preparation from $[\text{C}_6\text{H}_3\text{-}2,6\text{-(OP}^t\text{Bu}_2)_2\text{]Ir(H)Cl}$ (**1-HCl**) and sodium *tert*-butoxide in the presence isobutyronitrile (Figure 2).¹⁴ The iridium nitrile adduct was characterized by multinuclear NMR and infrared spectroscopy, as well as combustion analysis. The ³¹P{¹H} NMR spectrum of **1-NCⁱPr** in benzene-*d*₆ solution exhibits a single resonance at 178.9 ppm and an intense band at 2207 cm⁻¹ in the solution infrared spectrum.

In order to gain further insight into the pathway for catalytic amine dehydrogenation, a solution of **1-H₂** was treated with 3 equiv of TBE and isobutylamine and monitored by NMR spectroscopy at ambient temperature. After 30 min all **1-H₂** was completely consumed and two new species were observed (Figure 3). The ¹H NMR spectra of these new products are consistent with two C_{2v} symmetric molecules. In the minor product (~30%), resonances attributed to the amino and methyl protons of a bound molecule of isobutylamine were observed at 2.68 and 0.49 ppm, respectively. In addition a triplet (²J_{H-P}

= 16.4 Hz) of 2H intensity was detected at -8.84 ppm and assigned as an iridium hydride resonance. The minor product displays a singlet at 170.7 ppm in the ³¹P{¹H} NMR spectrum. This minor species was characterized as an iridium(III) amine dihydride complex,¹⁵ $[\text{C}_6\text{H}_3\text{-}2,6\text{-(OP}^t\text{Bu}_2)_2\text{]Ir(NH}_2^i\text{Bu)H}_2$ (**2**). The identity of **2** was confirmed via independent synthesis by addition of 2 equiv of isobutylamine to **1-H₂** in the absence of TBE. After 4 days at 23 °C, signals identical to those of complex **2** were observed as the major product, which was in equilibrium with **1-H₂** and the free amine.¹⁴ Attempts to isolate **2** by removal of the volatile materials resulted only in isolation of **1-H₂**.

The major product (~70%) observed in the **1-H₂**/TBE/isobutylamine reaction mixture after 30 min was assigned as the iridium(I) amine adduct $[\text{C}_6\text{H}_3\text{-}2,6\text{-(OP}^t\text{Bu}_2)_2\text{]Ir(NH}_2^i\text{Bu)}$ (**1-NH₂ⁱBu**) (Figure 3). An independent preparation of **1-NH₂ⁱBu** from $[\text{C}_6\text{H}_3\text{-}2,6\text{-(OP}^t\text{Bu}_2)_2\text{]Ir(H)Cl}$ and sodium *tert*-butoxide in the presence isobutylamine confirmed this assignment.¹⁴ This dark orange material was characterized by multinuclear NMR spectroscopy and elemental analysis. The ¹H NMR spectrum of **1-NH₂ⁱBu** exhibits resonances at 0.54 and 3.29 ppm, attributed to the amino and methyl protons of the bound amine, and a ³¹P{¹H} NMR resonance at 173.1 ppm.

Continued monitoring of the **1-H₂**/TBE/isobutylamine mixture at ambient temperature for 2.5 h resulted in complete conversion to **1-NH₂ⁱBu**. Allowing the reaction to proceed for an additional 19 h yielded small quantities (~10%) of **1-NCⁱPr**, which was observable by both ¹H and ³¹P{¹H} NMR spectroscopy. Complete consumption of **1-NH₂ⁱBu** was quite slow at ambient temperature and required warming of the solution to 60 °C over several days to achieve full conversion to **1-NCⁱPr**. Significantly, treatment with 10 additional equivalents of TBE did not increase the rate of **1-NCⁱPr** formation or effect detectable catalytic nitrile production at 60 °C.

Mechanism of Nitrile Synthesis. With the results of a preliminary investigation into the pathway for nitrile synthesis in hand, a proposed mechanism for the catalytic cycle was developed (Figure 4). In the presence of TBE and amine, an unproductive pre-equilibrium has been observed between precatalyst **1-H₂** and **2** (*vide supra*). However, upon thermolysis the mixture was proposed to convert swiftly and irreversibly to **1-NH₂ⁱBu**, driven by the hydrogenation of an equivalent of TBE. Based on reports from our laboratory¹⁶ and others,¹⁷ the iridium(I) amine adduct was proposed to equilibrate rapidly with an iridium(III) amido hydride species, with a strong thermodynamic preference for **1-NH₂ⁱBu**. The transient amido hydride complex was postulated to undergo β-hydride elimination, followed by hydrogenation of a TBE equivalent, to afford an iridium(I) imine adduct. The hydrogenation of TBE may be preceded by a ligand dissociation event, possibly the reversible loss of the bound imine ligand, as the proposed iridium(III) imine dihydride species is coordinatively saturated. Although a metal-imine complex was not observed during preliminary investigations into the dehydrogenation of isobutylamine, a related iridium(I) imine adduct has been isolated from the dehydrogenation of another primary amine (*vide infra*). Repetition of the N-H oxidative addition, β-hydride elimination, and

(11) Göttker-Schnetmann, I.; White, P.; Brookhart, M. *Organometallics* **2004**, *23*, 1766.

(12) Göttker-Schnetmann, I.; Brookhart, M. *J. Am. Chem. Soc.* **2004**, *126*, 9331.

(13) Successful catalytic amine dehydrogenation was observed at temperatures as low as 115 °C.

(14) See Experimental Section for details.

(15) Previous studies have indicated that donor ligands strongly disfavor formation of nonclassical Ir(I) dihydrogen complexes: Göttker-Schnetmann, I.; Heinekey, D. M.; Brookhart, M. *J. Am. Chem. Soc.* **2003**, *125*, 17114.

(16) Cartwright Sykes, A.; White, P.; Brookhart, M. *Organometallics* **2006**, *25*, 1664.

(17) (a) Kanzelberger, M.; Zhang, X.; Emge, T. J.; Goldman, A. S.; Zhao, J.; Incarvito, C.; Hartwig, J. F. *J. Am. Chem. Soc.* **2003**, *125*, 13644. (b) Zhao, J.; Goldman, A. S.; Hartwig, J. F. *Science (Washington, DC)* **2005**, *307*, 1080.

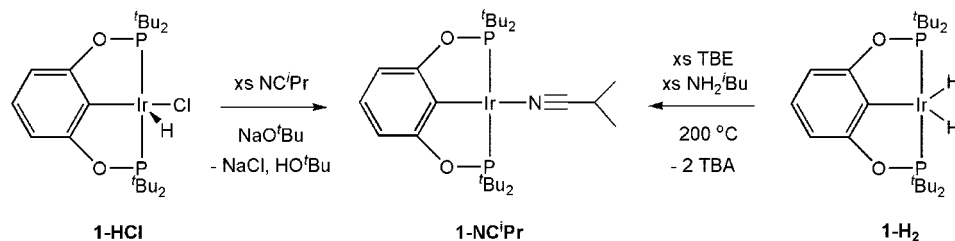


Figure 2. Pathways for the formation of nitrile adduct **1-NCⁱPr**.

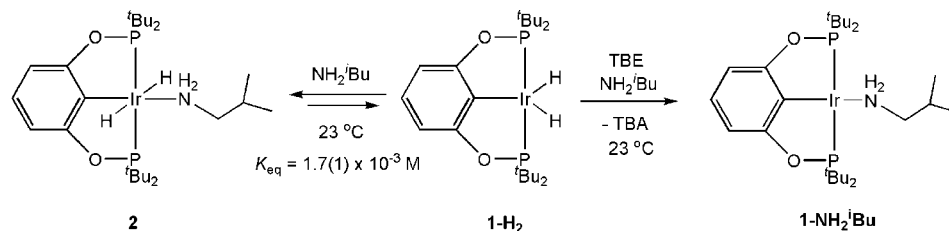


Figure 3. Formation of complexes **2** and **1-NH₂ⁱBu** from **1-H₂**.

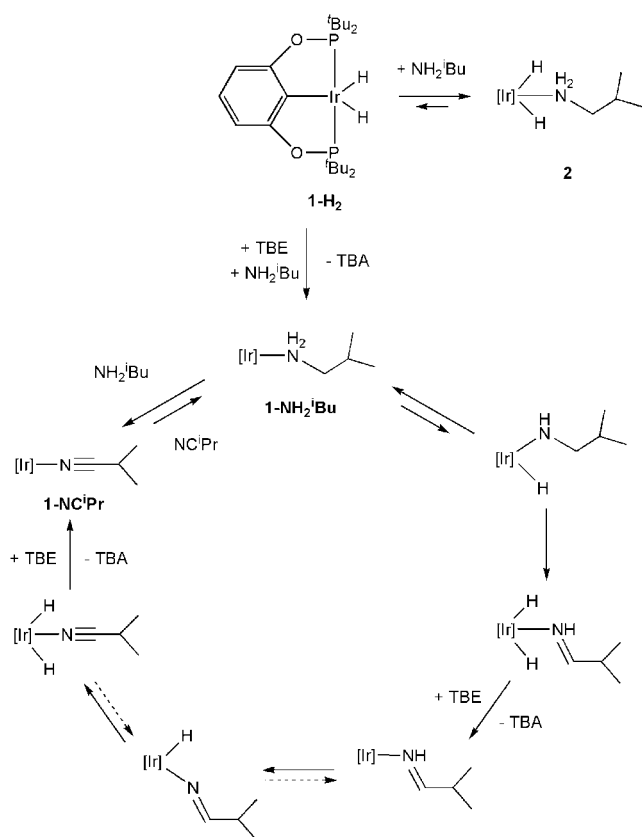


Figure 4. Proposed mechanism for the catalytic formation of isobutyronitrile.

TBE hydrogenation sequence from the iridium(I) imine species would afford the observed nitrile adduct **1-NCⁱPr**. Subsequent exchange of isobutylamine for the bound nitrile would re-form **1-NH₂ⁱBu** and complete the proposed catalytic cycle.

Following development of a mechanistic hypothesis, additional experiments were designed to further probe the catalytic pathway. Notably **1-NCⁱPr** was observed as the resting state during catalytic nitrile formation, although the amine adduct **1-NH₂ⁱBu** was also implicated as a reactive intermediate. This observation permitted study of the catalytic cycle in two component reactions: the stoichiometric transfer dehydrogenation of amine and the substitution of bound nitrile by amine.

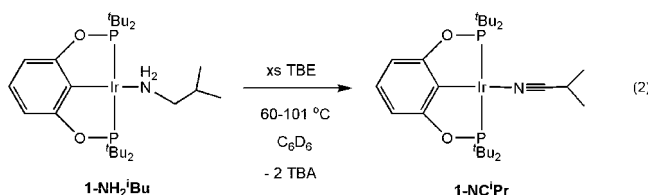
Table 1. Influence of [TBE] on the Rate Constant for **1-NH₂ⁱBu** Dehydrogenation^a

| [TBE] (M) | k_{obs} (s ⁻¹) |
|-----------|-------------------------------------|
| 0.279 | $2.1(1) \times 10^{-6}$ |
| 0.558 | $2.1(1) \times 10^{-6}$ |
| 0.837 | $2.0(1) \times 10^{-6}$ |

^a Rate constants measured for 0.0186 M benzene-*d*₆ solutions of **1-NH₂ⁱBu** at 60 °C.

To examine the mechanism of these component reactions in the amine transfer dehydrogenation cycle, a series of kinetic and isotopic labeling studies were performed.

Kinetics of the Dehydrogenation of 1-NH₂ⁱBu. The kinetics of stoichiometric transfer dehydrogenation of **1-NH₂ⁱBu** to **1-NCⁱPr** in the presence of TBE were monitored by ³¹P{¹H} NMR spectroscopy. In a typical experiment, a J. Young NMR tube was charged with a benzene-*d*₆ solution of **1-NH₂ⁱBu** and 15–45 equiv of TBE and heated (60–101 °C) for 1–7 days (eq 2).



To determine the order in [TBE], the observed rate constants for dehydrogenation were measured over several olefin concentrations while holding the initial concentration of **1-NH₂ⁱBu** constant. The results of these experiments are summarized in Table 1. No influence on the rate of **1-NH₂ⁱBu** dehydrogenation was observed over the investigated range of [TBE], affording an observed first-order rate constant of $2.1(1) \times 10^{-6} \text{ s}^{-1}$ at 60 °C.

The zero-order [TBE] dependence suggests that either N–H oxidative addition from **1-NH₂ⁱBu** or β -hydride elimination to form the iridium(III) imine dihydride complex likely occurs in the rate-limiting step for stoichiometric isobutylamine dehydrogenation (Figure 5). However a reversible β -hydride elimination event followed by a slow dissociation of imine prior to TBE hydrogenation could not be eliminated out of hand. This scenario was examined by monitoring the dehydrogenation of

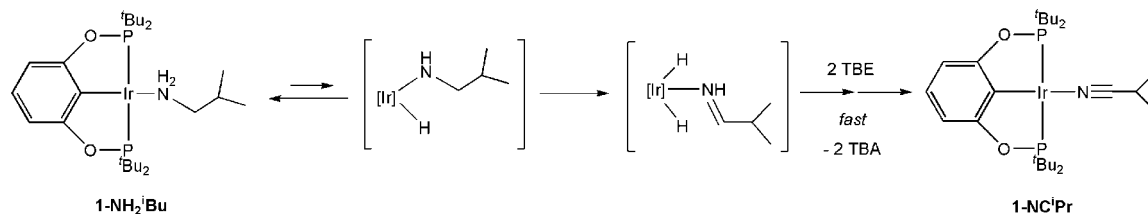


Figure 5. Proposed mechanism for the stoichiometric dehydrogenation of isobutylamine.

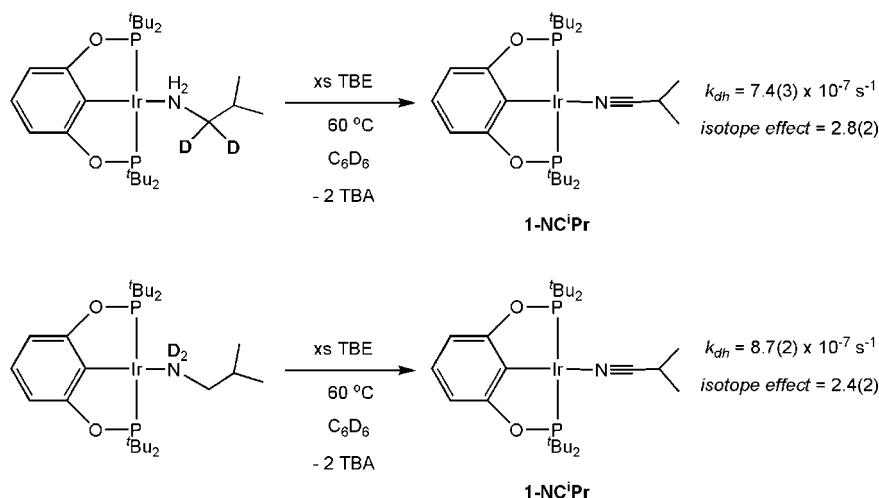


Figure 6. Isotopic labeling experiments for the dehydrogenation of **1-NH₂ⁱBu**.

the **1-NH₂ⁱBu** isotopologue, $[\text{C}_6\text{H}_3\text{-2,6-(OP}^i\text{Bu}_2)_2]\text{Ir}(\text{ND}_2^i\text{Bu})$.¹⁸ If the β -hydride elimination event were reversible, the deuterium labels on the amino position would be expected to scramble with those protons on the neighboring carbon center prior to nitrile formation.¹⁹ After $\sim 45\%$ conversion to **1-NCⁱPr** no scrambling of the deuterium label in $[\text{C}_6\text{H}_3\text{-2,6-(OP}^i\text{Bu}_2)_2]\text{Ir}(\text{ND}_2^i\text{Bu})$ was observed by either ^1H or ^2H NMR spectroscopy, thus rendering N–H oxidative addition or irreversible β -hydride elimination as the likely rate-limiting step of stoichiometric amine dehydrogenation.

These two mechanistic possibilities were distinguished by another set of isotopic labeling experiments. In one experiment a second isotopologue of **1-NH₂ⁱBu**, $[\text{C}_6\text{H}_3\text{-2,6-(OP}^i\text{Bu}_2)_2]\text{Ir}(\text{NH}_2\text{CD}_2\text{CH}(\text{CH}_3)_2)$, was dehydrogenated at 60 °C in the presence of 30 equiv of TBE with an observed rate constant of $7.4(3) \times 10^{-7} \text{ s}^{-1}$ (Figure 6).¹⁴ This reduced rate of reaction compared to the rate for the perprotio isotopologue afforded a kinetic isotope effect ($k_{\text{H}}/k_{\text{D}}$) of 2.8(2). In a similar experiment, $[\text{C}_6\text{H}_3\text{-2,6-(OP}^i\text{Bu}_2)_2]\text{Ir}(\text{ND}_2^i\text{Bu})$ was subjected to an identical dehydrogenation procedure (Figure 6) and yielded an observed rate constant of $8.7(2) \times 10^{-7} \text{ s}^{-1}$ at 60 °C with an isotope effect of 2.4(2).²⁰

The normal, primary isotope effect (secondary isotope effects are assumed to be small) observed for the dehydrogenation of

$[\text{C}_6\text{H}_3\text{-2,6-(OP}^i\text{Bu}_2)_2]\text{Ir}(\text{NH}_2\text{CD}_2\text{CH}(\text{CH}_3)_2)$ is consistent with activation of the C–D bond adjacent to the amino group occurring in the rate-limiting step for the formation of **1-NCⁱPr**. The kinetic isotope effect of 2.8(2) observed for this process is comparable to previously reported kinetic data for related iridium-mediated β -hydride elimination events.²¹ The observation of a significant isotope effect of 2.4(2) for the dehydrogenation of $[\text{C}_6\text{H}_3\text{-2,6-(OP}^i\text{Bu}_2)_2]\text{Ir}(\text{ND}_2^i\text{Bu})$ suggests a pre-rate-determining equilibrium in which the N–H(D) bond of the bound amine is ruptured.^{16,17} However it should be noted that the observed isotope effect is likely a composite of both equilibrium and kinetic isotope effects.²² Together with the zero-order dependence of [TBE] on the reaction rate, this set of isotopic labeling experiments is consistent with the following rate expression: $\text{rate} = k_{\text{dh}}[\mathbf{1-NH}_2^i\text{Bu}][\text{TBE}]^0$ for the stoichiometric dehydrogenation of isobutylamine.

Activation parameters for the dehydrogenation of **1-NH₂ⁱBu** to **1-NCⁱPr** were determined by measuring the observed rate constants for the reaction over a 41 °C temperature range. The effect of temperature on the rate of dehydrogenation is depicted in Figure 7, and the observed rate constants are reported in Table 2. From the Eyring plot an activation enthalpy (ΔH^\ddagger) of 24.8(9) kcal/mol and an activation entropy (ΔS^\ddagger) of $-10(2)$ eu were obtained. An activation enthalpy of this magnitude is consistent with considerable bond-breaking character in the rate-determining transition structure, as may be expected for a β -hydride

(18) Isotopically labeled amines were prepared as previously described: Friedman, L.; Jurewicz, A. T.; Bayless, J. H. *J. Am. Chem. Soc.* **1969**, *91*, 1795.

(19) Previous studies from our laboratory (ref 16) indicate that pincer iridium(III) amido hydride species adopt a square-pyramidal geometry with the amide ligand positioned in the basal plane. An iridium(III) imino dihydride product resulting from β -H elimination of such a species would then necessitate a *cis* orientation of the two hydride ligands with respect to the imine. This geometry would permit isotopic exchange of the Ir–H/N–H positions in a reversible process.

(20) Neglecting secondary kinetic isotope effects, an equilibrium isotope effect of this magnitude appears reasonable based on estimations using zero-point energy differences derived from Ir–H/Ir–D and N–H/N–D stretching frequencies.

(21) For examples of isotope effects for related β -H elimination events with iridium alkoxide complexes see: (a) Zhao, J.; Hesslink, H.; Hartwig, J. F. *J. Am. Chem. Soc.* **2001**, *123*, 7220. (b) Blum, O.; Milstein, D. *J. Am. Chem. Soc.* **1995**, *117*, 4582.

(22) For further discussions of equilibrium isotope effects at transition metal centers see: (a) Slaughter, L. M.; Wolczanski, P. T.; Klinckman, T. R.; Cundari, T. R. *J. Am. Chem. Soc.* **2000**, *122*, 7953. (b) Janak, K. E.; Parkin, G. *J. Am. Chem. Soc.* **2003**, *125*, 6889.

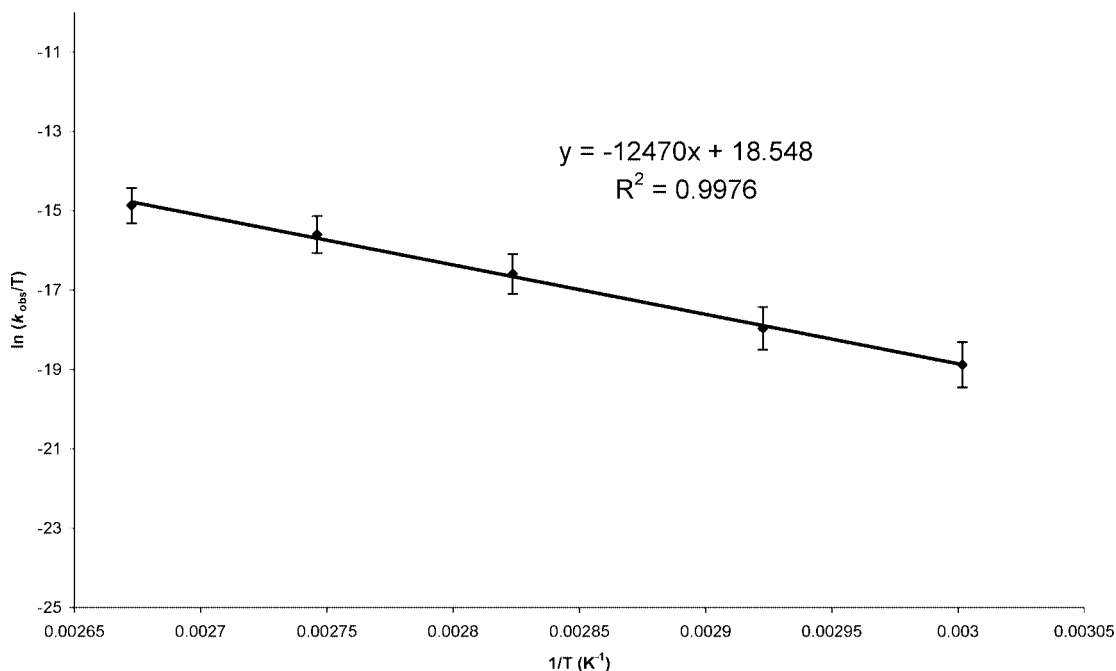


Figure 7. Eyring plot for the dehydrogenation of **1-NH₂ⁱBu**.

Table 2. Temperature Dependence of Rate Constants for **1-NH₂ⁱBu** Dehydrogenation^a

| T (K) | k _{obs} (s ⁻¹) |
|-------|-------------------------------------|
| 333 | 2.1(1) × 10 ⁻⁶ |
| 342 | 5.4(2) × 10 ⁻⁶ |
| 354 | 2.2(1) × 10 ⁻⁵ |
| 364 | 6.1(2) × 10 ⁻⁵ |
| 374 | 1.3(1) × 10 ⁻⁴ |

^a Rate constants measured for 0.0186 M benzene-*d*₆ solutions of **1-NH₂ⁱBu** with 30 equiv of TBE.

elimination event.²³ In addition, the relatively small entropy of activation would suggest a modestly ordered transition structure, consistent with a unimolecular process.²³ Overall, the Eyring plot affords a free energy activation barrier of 28(2) kcal/mol at 23 °C for stoichiometric isobutylamine dehydrogenation.

Kinetics of Nitrile Substitution. Observation of **1-NCⁱPr** as the resting state during catalytic dehydrogenation (*vide supra*) suggested that substitution of bound nitrile by amine was a significant step in the catalytic cycle. The substitution may either be the turnover-limiting step of nitrile formation or occur in an equilibrium prior to the turnover limiting step. Attempts to monitor the kinetics for substitution of **1-NCⁱPr** with isobutylamine were unsuccessful, as this reaction proceeded too slowly for convenient measurements at mild temperatures. Instead, the kinetics of the reverse reaction, substitution of bound amine by nitrile, were investigated by treating benzene-*d*₆ solutions of **1-NH₂ⁱBu** with 20 to 63 equiv of isobutyronitrile. The reaction progress was monitored by ³¹P{¹H} NMR spectroscopy and yielded clean first-order kinetic plots.²⁴

The effect of isobutyronitrile concentration on the rate of substitution was examined at 23 °C. The results are summarized in Table 3. Over a substantial range of [ⁱPrCN] the observed reaction rate remained unchanged, yielding a rate constant of 5.5(4) × 10⁻⁵ s⁻¹. This zero-order dependence on [ⁱPrCN]

Table 3. Influence of [ⁱPrCN] on the Rate Constant for **1-NH₂ⁱBu** Substitution^a

| [ⁱ PrCN] (M) | k _{obs} (s ⁻¹) |
|--------------------------|-------------------------------------|
| 0.344 | 5.7(4) × 10 ⁻⁵ |
| 0.508 | 5.8(4) × 10 ⁻⁵ |
| 0.937 | 5.1(4) × 10 ⁻⁵ |

^a Rate constants measured for 0.0175 M benzene-*d*₆ solutions of **1-NH₂ⁱBu** at 23 °C.

suggests that substitution of **1-NH₂ⁱBu** with nitrile (or the microscopic reverse, substitution of **1-NCⁱPr** with amine) may proceed via a dissociative or dissociative-interchange mechanism. Although associative substitution pathways for d⁸, square-planar transition metal complexes are more common,²⁵ recent reports on iridium pincer complexes have also shown substitution kinetics that are independent of ligand concentration.¹⁶ Rate constants for the substitution of **1-NH₂ⁱBu** with nitrile were also measured in the relatively noncoordinating solvents mesitylene-*d*₁₂ and cyclohexane-*d*₁₂ and found to be indistinguishable from those measured in benzene-*d*₆.²⁴ The absence of a substantial solvent effect on the rate of substitution renders a solvent-assisted pathway unlikely. The apparent dissociative or dissociative-interchange mechanism for nitrile/amine substitution may be imposed by the sterically demanding *tert*-butyl substituents on the pincer ligand. Overall, the kinetic data for the substitution of **1-NH₂ⁱBu** are consistent with the rate expression rate = k_{sub}[**1-NH₂ⁱBu**][ⁱPrCN]⁰.

The activation parameters for the reaction of **1-NH₂ⁱBu** with isobutyronitrile were also examined. The kinetic data and Eyring plot for the influence of temperature on the rate of substitution are presented in Table 4 and Figure 8, respectively. Analysis of these data yielded an activation enthalpy (ΔH[‡]) of 27(2) kcal/mol and activation entropy (ΔS[‡]) of 13(7) eu. In addition to the substantial enthalpy of activation, the positive activation

(23) (a) For related examples of activation parameters for β-hydride elimination see: Lu, C. C.; Peters, J. C. *J. Am. Chem. Soc.* **2004**, *126*, 15818. (b) Mueller, J. A.; Sigman, M. S. *J. Am. Chem. Soc.* **2003**, *125*, 7005. (c) Kovács, I.; Ungváry, F.; Markó, L. *Organometallics* **1994**, *13*, 1927.

(24) See Supporting Information for examples of kinetic plots.

(25) Jordan, R. B. *Reaction Mechanisms of Inorganic and Organometallic Systems*, 2nd ed.; Oxford University Press: New York, 1998; pp 25–32.

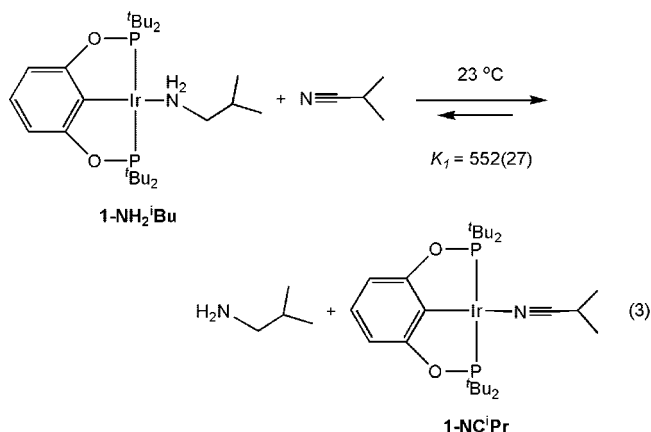
Table 4. Temperature Dependence of Rate Constants for 1-NH₂^tBu Substitution^a

| <i>T</i> (K) | <i>k</i> _{obs} (s ⁻¹) |
|--------------|--|
| 281 | 3.1(3) × 10 ⁻⁶ |
| 288 | 1.2(2) × 10 ⁻⁵ |
| 297 | 5.7(4) × 10 ⁻⁵ |
| 305 | 2.3(2) × 10 ⁻⁴ |
| 320 | 1.4(2) × 10 ⁻³ |

^a Rate constants measured for 0.0175 M benzene-*d*₆ solutions of **1-NH₂^tBu** with 20 equiv of [PrCN].

entropy further supports a dissociative substitution process,²⁶ which proceeds with an activation barrier of 23(1) kcal/mol at 23 °C.

Although the barrier for substitution of **1-NC^tPr** with isobutylamine could not be measured directly, the thermodynamic binding preference for nitrile versus amine was measured and used to compute this activation energy. A solution of **1-NC^tPr** was treated with a large excess of isobutylamine (> 175 equiv) and allowed to approach equilibrium with **1-NH₂^tBu** and isobutyronitrile at 23 °C over the course of several weeks.¹⁴ Quantitative analysis by NMR spectroscopy afforded an equilibrium constant (*K*₁) of 552(27) at 23 °C (eq 3).



Attempts to approach this equilibrium by addition of isobutyronitrile to **1-NH₂^tBu** yielded quantities of residual nitrile and **1-NH₂^tBu** that were too small for reliable quantification. The strong preference for iridium to bind isobutyronitrile over isobutylamine represents a 3.7(4) kcal/mol ground-state stabilization of **1-NC^tPr**/amine compared to **1-NH₂^tBu**/nitrile at 23 °C (Figure 9). When taken together with the experimentally measured barrier of 23(1) kcal/mol, the equilibrium constant (*K*₁) permits calculation of an activation barrier of 27(2) kcal/mol at 23 °C for the substitution of **1-NC^tPr** by isobutylamine.²⁷

Mechanistic Considerations for Catalytic Isobutylamine Dehydrogenation. Analysis of the activation barriers for the component reactions, stoichiometric amine dehydrogenation from **1-NH₂^tBu** ($\Delta G_{\text{dh}}^{\ddagger}$ 28(2) kcal/mol) and nitrile substitution from **1-NC^tPr** (ΔG_1^{\ddagger} = 27(2) kcal/mol) at 23 °C suggests that these two processes proceed with similar rates. However the relatively low barrier to substitution of **1-NH₂^tBu** with free nitrile (ΔG_{-1}^{\ddagger} = 23(1) kcal/mol) compared to that for amine

Table 5. Substrates for Catalytic Amine Dehydrogenation^a

| substrate | conversion (%) ^b | | |
|--|-----------------------------|------|------|
| | 15 h | 30 h | 45 h |
| isobutylamine | 44 | 76 | 80 |
| <i>p</i> -methoxybenzylamine | 78 | 87 | 93 |
| <i>p</i> -methylbenzylamine | 60 | 75 | 85 |
| benzylamine | 57 | 75 | 84 |
| <i>p</i> -(trifluoromethyl)benzylamine | 34 | 38 | 39 |
| <i>p</i> -chlorobenzylamine | <5 | 12 | 17 |

^a Conditions: 5 mol % **1-H₂** in mesitylene-*d*₁₂, 5:1 [TBE]:[amine], 185 °C. ^b Conversions were determined by *in situ* NMR spectroscopy.

dehydrogenation indicates that nitrile substitution should be reversible during catalytic amine dehydrogenation. Due to the positive entropy of activation for the dissociative substitution process, this effect is magnified at the elevated temperatures required for catalytic turnover (Figure 10). A $\Delta\Delta G^{\ddagger}$ = 8 kcal/mol (185 °C) between β -hydride elimination and substitution of bound amine may be extrapolated from the respective Eyring parameters. Although the barrier to substitution of **1-NC^tPr** with isobutylamine (ΔG_1^{\ddagger}) could not be obtained under these conditions, the available kinetic data implicate a catalytic amine dehydrogenation cycle consistent with that depicted in Figure 11.

Mechanistic data suggest that catalytic amine dehydrogenation proceeds via a turnover-limiting β -hydride elimination step following two rate-influencing pre-equilibria. A reversible substitution of amine for nitrile at the catalyst resting state, **1-NC^tPr**, is followed by reversible N–H bond oxidative addition. The observation of **1-NC^tPr** as the only detectable iridium species under catalytic conditions suggests that both pre-equilibria are established rapidly and favor the nitrile adduct. The slow β -hydride elimination to form a bound imine species is then followed by a rapid sequence of TBE hydrogenation and imine dehydrogenation events to re-form **1-NC^tPr**.

Simplification of the complex rate law for catalytic amine dehydrogenation using either the equilibrium approximation²⁸ or the method of determinants²⁹ affords the rate expression in eq 4.

$$\frac{d[\text{PrCN}]}{dt} = \frac{k_{\text{obs}}[\mathbf{1-PrCN}][\text{NH}_2\text{Bu}]}{[\text{PrCN}]}; \text{ where } k_{\text{obs}} = \frac{k_1 k_2 k_3}{k_{-1} k_{-2}} \quad (4)$$

The full rate expression for the amine dehydrogenation as well as the derivation of eq 4 is detailed in the Supporting Information. The rate of nitrile formation bears a first-order dependence on the total concentration of iridium in the reaction ([Ir]_{tot}). Following the rapid activation of **1-H₂** with TBE, [Ir]_{tot} should be approximately equal to [1-PrCN] under catalytic conditions. Significantly, the simplified rate expression indicates an inverse first-order dependence on free nitrile, suggesting that product inhibition may diminish nitrile production at high conversions. To investigate the validity of these mechanistic implications, a small collection of primary amines were catalytically oxidized to nitriles.

Substrates for Catalytic Amine Dehydrogenations. To ascertain the influence of electron-withdrawing or -donating groups on substrates for catalytic amine dehydrogenation, a series of *para*-substituted benzyl amines was dehydrogenated. The results of these studies as well as data for the dehydrogenation of isobutylamine are summarized in Table 5. Catalytic

(26) Maskill, H. *The Physical Basis of Organic Chemistry*; Oxford Science Publications: New York, 1985; pp 216–314.

(27) (a) For a discussion of this method for the determination of dissociation activation energies see: Bryndza, H. E.; Domaille, P. J.; Paciello, R. A.; Bercaw, J. E. *Organometallics* **1989**, *8*, 379. (b) Asali, K. J.; Awad, H. H.; Kimbrough, J. F.; Lang, B. C.; Watts, J. M.; Dobson, G. R. *Organometallics* **1991**, *10*, 1822. (c) Klassen, J. K.; Selke, M.; Sorensen, A. A.; Yang, G. K. *J. Am. Chem. Soc.* **1990**, *112*, 1267.

(28) Collman, J. P.; Hegedus, L. S.; Norton, J. R.; Finke, R. G. *Principles and Application of Organotransition Metal Chemistry*; University Science Books: Sausalito, 1987; pp 235–278.

(29) King, E. L.; Altman, C. *J. Phys. Chem.* **1956**, *60*, 1375.

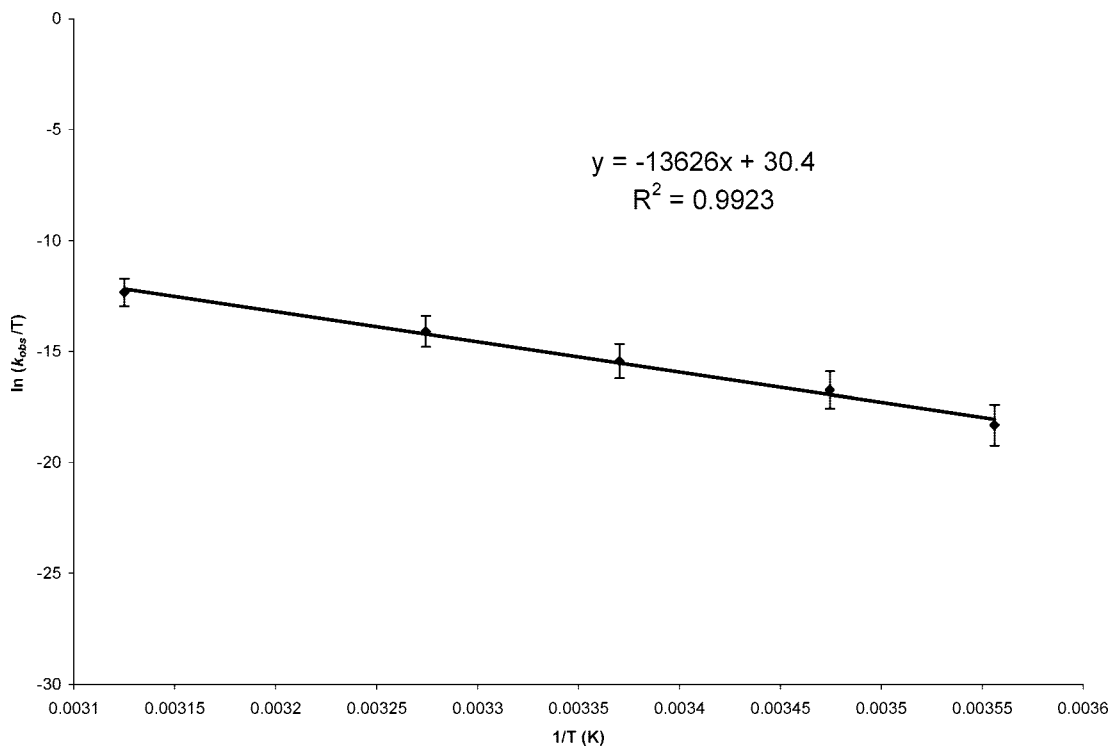


Figure 8. Eyring plot for the substitution of **1-NH₂^tBu** with isobutyronitrile.

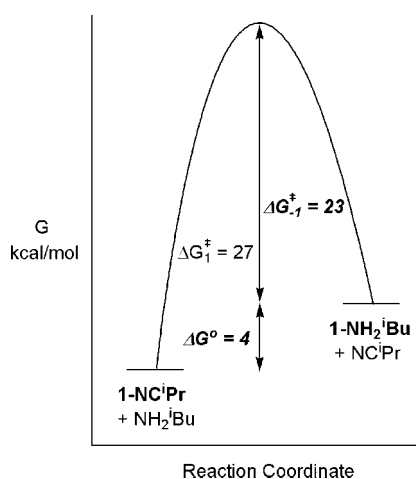


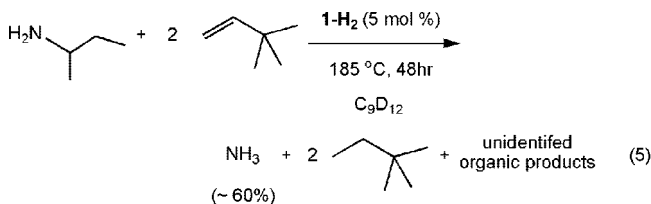
Figure 9. Free energy diagram for the competitive binding of amine and nitrile to pincer iridium at 23 °C. Energies derived from experimental data are presented in italics.

dehydrogenations were carried out at 185 °C in mesitylene-*d*₁₂ using 5 mol % of **1-H₂** and a 5:1 ratio of TBE to amine. Conversion of the amine to nitrile was monitored by NMR spectroscopy.¹⁴ Those benzyl amines bearing electron-donating groups (entries 2 and 3) underwent more facile dehydrogenation relative to amines substituted with electron-withdrawing groups (entries 5 and 6). The parent benzyl amine (entry 4) converted at a rate intermediate between these two substituent types.

The enhanced catalytic conversion of amine substrates bearing electron-donating substituents is consistent with the mechanistic description proposed in Figures 10 and 11. The presence of electron-donating groups on the amine and subsequent nitrile may be expected to enhance product inhibition by generating a strongly bound iridium(I) nitrile adduct. However, the highest barrier on the reaction coordinate was proposed to occur during β -hydride elimination from the transient iridium(III) amido hydride species. It has previously been reported that electron-

donating substituents at the *para* position lower the bond dissociation enthalpy of benzylic C–H bonds, in this case, the bond to be broken during formation of the bound imine.³⁰ Thus, the data in Table 5 suggest that substituent effects favoring β -hydride elimination dominate over those influencing nitrile substitution.

The successful dehydrogenation of primary amines to free nitriles offered the prospect of also producing imines from –NH₂-substituted secondary carbon centers. Unfortunately the limited stability of imines formed from primary amines has hampered this approach.³¹ Treatment of **1-H₂** with 10 equiv of *sec*-butylamine and 20 equiv of TBE at 185 °C in mesitylene-*d*₁₂ for 48 h afforded significant quantities of ammonia (~60% based on the amine), TBA, and several unidentified organic species. Residual amine in a quantity of <10% as judged by ¹H NMR spectroscopy was also observed (eq 5).



Significantly, no free imine, HN=C(CH₃)(CH₂CH₃), was detected in this reaction mixture. Analysis of the residual organometallic species revealed the formation of two isomers of {C₆H₃-2,6-[OP(^tBu)₂]₂}Ir(HN=C(Me)Et) (**3**), which were identified by multinuclear one- and two-dimensional NMR spectroscopy and combustion analysis (Figure 12).¹⁴

(30) Nam, P.; Nguyen, M. T.; Chandra, A. K. *J. Phys. Chem. A* **2005**, *109*, 10342.

(31) (a) Crampton, M. R.; Lord, S. D.; Millar, R. *Perkin Trans. 2* **1997**, 909. (b) Boyd, D. R.; Coulter, P. B.; Hamilton, R.; Thompson, N. T.; Sharma, N. D.; Stubbs, M. E. *Perkin Trans. 1* **1985**, 2123.

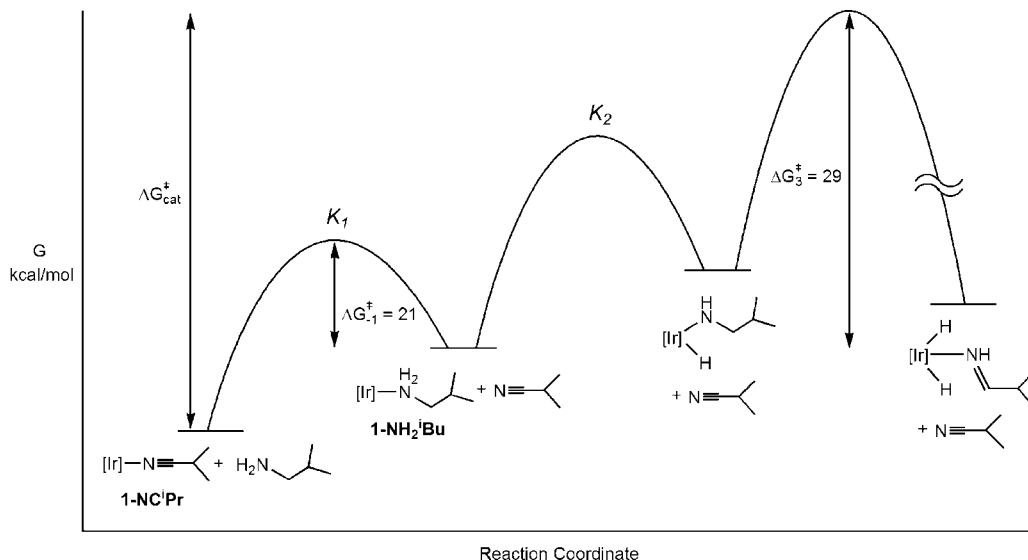


Figure 10. Free energy diagram for the kinetically significant transformations of catalytic isobutylamine dehydrogenation at 185 °C.

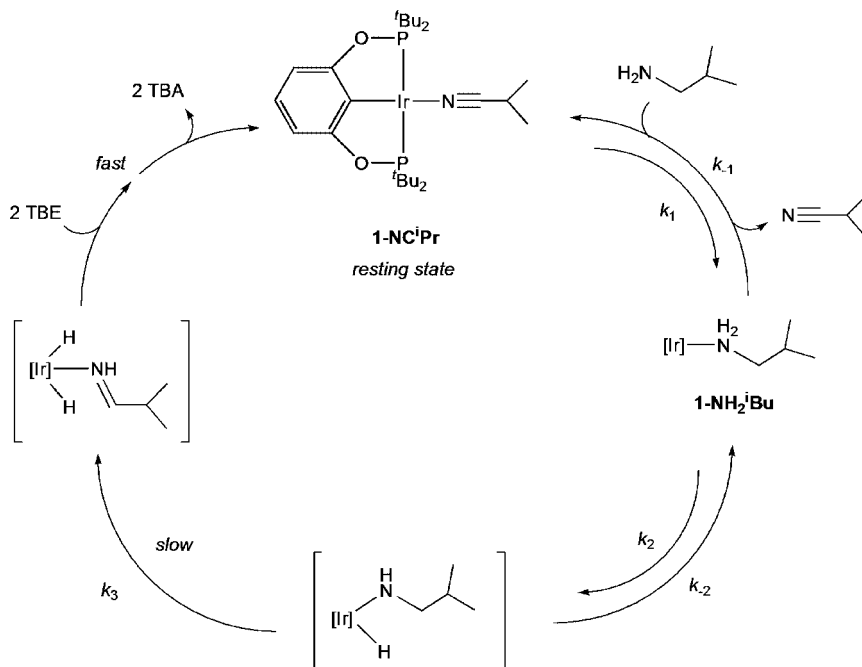


Figure 11. Proposed cycle for the catalytic dehydrogenation of isobutylamine.

The *E*-isomer of complex **3** was slightly favored (1.6:1) over the *Z*-isomer in an equilibrated benzene-*d*₆ solution at 23 °C. An isomeric mixture of bound imines derived from *sec*-butylamine have also been reported for tungsten(II) complexes.³² Assignment of the two isomers was accomplished by 2D NOESY NMR spectroscopy, which indicated a through-space correlation between the N–H and N=C–CH₃ resonances of the minor isomer, but not in the major isomer. This correlation suggests a *cis* orientation of the N–H bond and the methyl group alpha to the imine carbon, thus indicating the minor product is the *Z*-isomer. Significantly, the isolation of the imine adduct **3** does provide circumstantial support for the intermediacy of similar complexes proposed during catalytic nitrile production from primary amines (Figure 4).

The conversion of *sec*-butylamine to ammonia and other organics, as well as the isolation of complex **3**, suggests that catalytic dehydrogenation of the amine may occur. However the imine product may be unstable under the conditions required for catalytic transformation. The presence of ammonia in the product mixture is consistent with previously described degradation pathways for N–H-substituted imines.³¹ Unfortunately, attempts to dehydrogenate *sec*-butylamine under more mild conditions yielded no catalytic transformation.

Concluding Remarks

The mechanism of amine dehydrogenation catalyzed by **1-H**₂ has been explored by a series of kinetic and isotopic labeling experiments. The catalytic cycle was examined using isobutylamine in two stoichiometric component reactions: (1) dehydro-

(32) Francisco, L. W.; White, P. S.; Templeton, J. L. *Organometallics* 1996, 15, 5127.

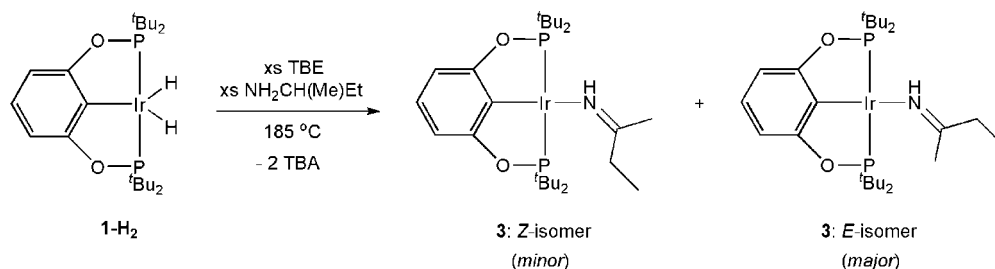


Figure 12. Formation of the isomers of complex **3**.

generation of the iridium(I) amine adduct, **1-NH₂^tBu**, to the iridium(I) nitrile complex, **1-ⁱPrCN**, and (2) the substitution of **1-ⁱPrCN** with isobutylamine. The kinetics of **1-NH₂^tBu** dehydrogenation were consistent with a reversible N–H oxidative addition followed by a slow β -hydride elimination event from a transient iridium(III) amido hydride species. Subsequent steps to afford the nitrile complex **1-ⁱPrCN** proceed rapidly with no dependence on the concentration of sacrificial olefin for the catalytic turnover rate.

The reversible interchange of **1-ⁱPrCN**/isobutylamine and **1-NH₂^tBu**/isobutyronitrile displays a strong thermodynamic preference for formation of the nitrile adduct. Kinetic studies indicated no dependence on the concentration of the incoming ligand on the rate of substitution. Activation parameters of $\Delta H^\ddagger = 24.8(9)$ kcal/mol and $\Delta S^\ddagger = -10(2)$ eu for the substitution of **1-NH₂^tBu** with isobutyronitrile were also consistent with a dissociative or dissociative-interchange pathway. Although the barriers for stoichiometric amine dehydrogenation and nitrile substitution are comparable near ambient temperature, β -hydride elimination during amine dehydrogenation was proposed to dominate the reaction coordinate under catalytic conditions. Catalytic dehydrogenation is believed to proceed via two pre-turnover-limiting equilibria from the resting state, a nitrile adduct, followed by slow β -hydride elimination from a transient iridium(III) amido hydride species.

The proposed mechanistic pathway for amine oxidation was also supported by the reactivity as a series of *para*-substituted benzyl amines. The enhanced conversion observed for amines bearing electron-donating substituents is consistent with a dominating influence of β -hydride elimination during amine dehydrogenation. Additionally, attempts to dehydrogenate the primary amine of a secondary carbon center afforded an iridium(I) imine complex, analogous to a proposed intermediate for catalytic nitrile synthesis. Under the conditions required for catalytic dehydrogenation, the N–H-substituted imine products were unstable. Further studies of the dehydrogenation of functionalized organic molecules are currently ongoing in our laboratory. Development of these methods may lead to improved yields for catalytic amine dehydrogenations as well as new techniques for the mild oxidation of other classes of organic molecules.

Experimental Section

General Considerations. All manipulations were carried out using standard vacuum, Schlenk, cannula, or glovebox techniques. Argon gas was purified by passage through columns of BASF R3-11 and 4 Å molecular sieves. THF was distilled from sodium benzophenone ketyl under nitrogen. Benzene-*d*₆ and cyclohexane-*d*₁₂ were dried over 4 Å molecular sieves and distilled prior to use. Mesitylene-*d*₁₂ was passed through a plug of activated neutral alumina prior to use. All amines and nitriles were purchased from Aldrich, Acros, or TCI Chemicals, dried over CaH₂, and distilled prior to use. *tert*-Butylethylene was purchased from Aldrich and

dried over sodium metal and distilled prior to use. All other solvents were dried and deoxygenated using literature procedures.³³

¹H, ¹³C, and ³¹P NMR spectra were recorded on Bruker DRX 400 and 500 MHz spectrometers. ¹H and ¹³C chemical shifts are referenced to residual protio solvent signals; ³¹P chemical shifts are referenced to an external standard of H₃PO₄. Probe temperatures were calibrated using ethylene glycol and methanol as previously described.³⁴ Due to strong ³¹P–³¹P coupling in the pincer ligand, many ¹H and ¹³C NMR signals appear as virtual triplets (vt) and are reported as such with the apparent coupling noted. IR spectra were recorded on an ASI React IR 1000 spectrometer. Elemental analyses were performed at Robertson MicroLit Laboratories, Inc., in Madison, NJ.

General Procedure for the Determination of Kinetics of 1-NH₂^tBu Dehydrogenation. A J. Young NMR tube was charged with 500 mg of a benzene-*d*₆ solution of **1-NH₂^tBu** (or appropriate isotopologue) of known concentration (0.0125–0.0175 M). Then 15, 30, or 45 equiv of *tert*-butylethylene were added via microsyringe. The contents of the tube were sealed under argon and heated (60–101 °C) by submersion in a constant temperature bath. Although kinetic measurements suggest no rate dependence on the concentration of *tert*-butylethylene, the volatile olefin was always used in large excess to ensure a sufficient concentration in solution at all times. The reaction progress was monitored by ³¹P NMR spectroscopy over approximately 2 half-lives. The decay of the resonance for **1-NH₂^tBu** was converted to concentration and fitted to first-order plots of ln [**1-NH₂^tBu**] versus time, which gave observed rate constants as the slope. Examples of these graphs can be found in the Supporting Information.

General Procedure for the Determination of Kinetics of 1-NH₂^tBu Substitution by Nitrile. A J. Young NMR tube was charged with 500 mg of a benzene-*d*₆ solution of **1-NH₂^tBu** of known concentration (0.0125–0.0300 M). Then 20, 32, and 63 equiv of isobutyronitrile were added via microsyringe. The reaction progress (8–47 °C) was monitored by ³¹P NMR spectroscopy over approximately 2 half-lives. The decay of the resonance for **1-NH₂^tBu** was converted to concentration and fitted to pseudo-first-order plots of ln [**1-NH₂^tBu**] versus time, which gave observed rate constants as the slope. Examples of these graphs can be found in the Supporting Information.

Procedure for the Determination of the Equilibrium Constants. Equilibration of 1-H₂/isobutylamine and 2. A J. Young NMR tube was charged with 5 mg of **1-H₂**, 11 Torr in 28.9 mL of isobutylamine vapor, and 489 mg of benzene-*d*₆. The reaction was then monitored by NMR spectroscopy over 1 week at 23 °C, yielding concentrations as follows: [^tBuNH₂] = 0.0048 M, [**1-H₂**] = 0.0044 M, [**2**] = 0.0121 M.

Equilibration of 1-NCⁱPr/isobutylamine and 1-NH₂^tBu/isobutyronitrile. A J. Young NMR tube was charged with 9 mg of **1-NCⁱPr**, 250 μ L of isobutylamine, and 427 mg of benzene-*d*₆. The reaction was then monitored by NMR spectroscopy over 6

(33) Pangborn, A. B.; Giardello, M. A.; Grubbs, R. H.; Rosen, R. K.; Timmers, F. J. *Organometallics* **1996**, *15*, 1518.

(34) Sandström, J. *Dynamic NMR Spectroscopy*; Academic Press: New York, 1982.

weeks at 23 °C, yielding concentrations as follows: $[\text{t-BuNH}_2] = 3.557 \text{ M}$, $[\text{NC}^i\text{Pr}] = 0.008 \text{ M}$, $[\mathbf{1-NC}^i\text{Pr}] = 0.011 \text{ M}$, $[\mathbf{1-NH}_2^i\text{Bu}] = 0.008 \text{ M}$.

General Procedure for the Catalytic Dehydrogenation of Amines to Nitriles. A J. Young NMR tube was charged with 5 mg of $\mathbf{1-H}_2$ and 400 mg of mesitylene- d_{12} . Then 20 equiv of amine and 100 equiv of *tert*-butylethylene were added via microsyringe. The reaction was heated at 185 °C for 45 h. Conversion was monitored by NMR spectroscopy, and the products were identified by comparison to authentic samples.

Preparation of $\{\text{C}_6\text{H}_3\text{-2,6-[OP}^i(\text{Bu})_2\text{]}_2\}\text{Ir}(\text{N}\equiv\text{C}^i\text{Pr})$ ($\mathbf{1-NC}^i\text{Pr}$).
Method A: A 25 mL Schlenk flask was charged with 0.100 g (0.160 mmol) of $\{\text{C}_6\text{H}_3\text{-2,6-[OP}^i(\text{Bu})_2\text{]}_2\}\text{Ir}(\text{H})\text{Cl}$ ($\mathbf{1-HCl}$)¹⁰ and 0.018 g (0.188 mmol) of sodium *tert*-butoxide. On a vacuum line, 1.0 mL (11.00 mmol) of isobutyronitrile and approximately 10 mL of toluene were vacuum transferred into the Schlenk flask at -196 °C. The solution was allowed to warm slowly to ambient temperature and stirred for 4 h. The solvent and excess nitrile were removed *in vacuo* from the orange reaction mixture. The residue was then extracted with pentane, filtered through Celite, and recrystallized at -35 °C to afford 0.088 g (84%) of $\mathbf{1-NC}^i\text{Pr}$ as orange blocks.

Method B: A heavy-walled glass reaction vessel was charged with 0.025 g (0.042 mmol) of $\{\text{C}_6\text{H}_3\text{-2,6-[OP}^i(\text{Bu})_2\text{]}_2\}\text{IrH}_2$ ($\mathbf{1-H}_2$)¹¹ and approximately 10 mL of toluene. On a vacuum line, 3 equiv (0.126 mmol) of isobutylamine and *tert*-butylethylene were added via a calibrated gas bulb (81 Torr in 28.9 mL) at -196 °C. The solution was heated at 185 °C for 18 h, and the volatiles were removed *in vacuo*. The residue was extracted with diethyl ether, filtered through Celite, and recrystallized at -35 °C to afford 0.020 g (57%) of $\mathbf{1-NC}^i\text{Pr}$ as orange blocks. Anal. Calcd for $\text{C}_{26}\text{H}_{46}\text{IrNP}_2\text{O}_2$: C, 47.40; H, 7.04; N, 2.13. Found: C, 47.11; H, 7.20; N, 2.07. ¹H NMR (23 °C, C_6D_6): δ 0.64 (d, 7.4 Hz, 6H, $\text{N}\equiv\text{CCH}(\text{CH}_3)_2$), 1.48 (vt, 6.6 Hz, 36H, $\text{P-C}(\text{CH}_3)_3$), 1.89 (sept, 7.4 Hz, 1H, $\text{N}\equiv\text{CC} \text{H}(\text{CH}_3)_2$), 6.91–6.99 (m, 3H, C_6H_3). ³¹P{¹H} NMR (23 °C, C_6D_6): δ 178.9. ¹³C{¹H} NMR (23 °C, C_6D_6): δ 19.41 ($\text{N}\equiv\text{CCH}(\text{CH}_3)_2$), 22.61 ($\text{N}\equiv\text{CCH}(\text{CH}_3)_2$), 28.86 (vt, 3.7 Hz, $\text{P-C}(\text{CH}_3)_3$), 41.72 (vt, 11.0 Hz, $\text{P-C}(\text{CH}_3)_3$), 104.14, 123.11, 136.77, 169.66 (C_6H_3), 133.13 (N^iC). IR (pentane): $\nu_{\text{N}=\text{C}} = 2207 \text{ cm}^{-1}$.

Preparation of $\{\text{C}_6\text{H}_3\text{-2,6-[OP}^i(\text{Bu})_2\text{]}_2\}\text{Ir}(\text{NH}_2^i\text{Bu})$ ($\mathbf{1-NH}_2^i\text{Bu}$).
 A 25 mL Schlenk flask was charged with 0.050 g (0.080 mmol) of $\{\text{C}_6\text{H}_3\text{-2,6-[OP}^i(\text{Bu})_2\text{]}_2\}\text{Ir}(\text{H})\text{Cl}$ ($\mathbf{1-HCl}$)¹⁰ and 0.010 g (0.104 mmol) of sodium *tert*-butoxide. On a vacuum line, 0.5 mL (4.924 mmol) of isobutylamine and approximately 10 mL of toluene were vacuum transferred into the Schlenk flask at -196 °C. The solution was allowed to warm slowly to ambient temperature and stirred for 4 h. The solvent and excess amine were removed *in vacuo* from the dark orange reaction mixture. The residue was then extracted with pentane, filtered through Celite, and recrystallized at -35 °C to afford 0.039 g (74%) of $\mathbf{1-NH}_2^i\text{Bu}$ as orange blocks. Anal. Calcd for $\text{C}_{26}\text{H}_{50}\text{IrNP}_2\text{O}_2$: C, 47.11; H, 7.60; N, 2.11. Found: C, 46.88; H, 7.37; N, 2.12. ¹H NMR (23 °C, C_6D_6): δ 0.54 (d, 7.4 Hz, 6H, $\text{NH}_2\text{CH}_2\text{CH}(\text{C} \text{H}_3)_2$), 1.07 (m, 1H, $\text{NH}_2\text{CH}_2\text{C} \text{H}(\text{CH}_3)_2$), 1.37 (vt, 6.8 Hz, 36H, $\text{P-C}(\text{C} \text{H}_3)_3$), 2.71 (m, 2H, $\text{NH}_2\text{CH}_2\text{CH}(\text{CH}_3)_2$), 3.29 (m, 2H, $\text{N} \text{H}_2\text{CH}_2\text{CH}(\text{CH}_3)_2$), 6.86 (d, 7.6 Hz, 2H, $m\text{-C}_6\text{H}_3$), 6.98 (t, 7.6 Hz, 1H, $p\text{-C}_6\text{H}_3$). ³¹P{¹H} NMR (23 °C, C_6D_6): δ 173.1.

¹³C{¹H} NMR (23 °C, C_6D_6): δ 19.56 ($\text{NH}_2\text{CH}_2\text{CH}(\text{CH}_3)_2$), 29.12 (vt, 3.6 Hz, $\text{P-C}(\text{CH}_3)_3$), 32.57 ($\text{NH}_2\text{CH}_2\text{CH}(\text{CH}_3)_2$), 41.62 (vt, 10.9 Hz, $\text{P-C}(\text{CH}_3)_3$), 59.77 ($\text{NH}_2\text{CH}_2\text{CH}(\text{CH}_3)_2$), 103.70, 121.41, 130.54, 168.08 (C_6H_3).

Observation of $\{\text{C}_6\text{H}_3\text{-2,6-[OP}^i(\text{Bu})_2\text{]}_2\}\text{IrH}_2(\text{NH}_2^i\text{Bu})$ ($\mathbf{2}$). A J. Young NMR tube was charged with 0.005 g (0.008 mmol) of $\{\text{C}_6\text{H}_3\text{-2,6-[OP}^i(\text{Bu})_2\text{]}_2\}\text{IrH}_2$ ($\mathbf{1-H}_2$)¹¹ and 0.489 g of benzene- d_6 . On a vacuum line, 1 equiv of isobutylamine was admitted at -196 °C via calibrated gas bulb (6 Torr in 28.9 mL). The equilibration of $\mathbf{1-H}_2$ and $\mathbf{2}$ was monitored over 4 days by NMR spectroscopy, affording a ratio of 1:2.8 of metal complexes at 23 °C. Complex $\mathbf{2}$: ¹H NMR (23 °C, C_6D_6): δ -8.84 (t, 16.4 Hz, 2H, Ir-H), 0.49 (d, 7.4 Hz, 6H, $\text{NH}_2\text{CH}_2\text{CH}(\text{CH}_3)_2$), 0.94 (m, 1H, $\text{NH}_2\text{CH}_2\text{CH}(\text{CH}_3)_2$), 1.46 (vt, 6.8 Hz, 36H, $\text{P-C}(\text{CH}_3)_3$), 2.59 (m, 2H, $\text{NH}_2\text{CH}_2\text{-CH}(\text{CH}_3)_2$), 2.68 (m, 2H, $\text{NH}_2\text{CH}_2\text{CH}(\text{CH}_3)_2$), 6.71 (d, 7.6 Hz, 2H, $m\text{-C}_6\text{H}_3$), 6.80 (t, 7.6 Hz, 1H, $p\text{-C}_6\text{H}_3$). ³¹P{¹H} NMR (23 °C, C_6D_6): δ 170.7.

Preparation of $\{\text{C}_6\text{H}_3\text{-2,6-[OP}^i(\text{Bu})_2\text{]}_2\}\text{Ir}(\text{HN}=\text{C}(\text{Me})\text{Et})$ ($\mathbf{3}$). A heavy-walled glass reaction vessel was charged with 0.025 g (0.042 mmol) of $\{\text{C}_6\text{H}_3\text{-2,6-[OP}^i(\text{Bu})_2\text{]}_2\}\text{IrH}_2$ ($\mathbf{1-H}_2$)¹¹ and approximately 5 mL of toluene. On a vacuum line, 3 equiv (0.126 mmol) of *sec*-butylamine and *tert*-butylethylene were added via a calibrated gas bulb (81 Torr in 28.9 mL) at -196 °C. The solution was heated at 185 °C for 18 h, and the volatiles were removed *in vacuo*. The residue was extracted with pentane, filtered through Celite, and recrystallized at -35 °C to afford 0.016 g (71%) as an orange powder. Anal. Calcd for $\text{C}_{26}\text{H}_{48}\text{IrNP}_2\text{O}_2$: C, 47.26; H, 7.32; N, 2.12. Found: C, 47.05; H, 7.39; N, 1.99. Characterization data for the *E*-isomer (*major*): ¹H NMR (23 °C, C_6D_6): δ 0.55 (t, 7.6 Hz, 3H, $\text{HN}=\text{C}(\text{CH}_3)\text{CH}_2\text{C} \text{H}_3$), 1.36 (vt, 6.4 Hz, 36H, $\text{P-C}(\text{C} \text{H}_3)_3$), 1.41 (q, 7.6 Hz, 2H, $\text{HN}=\text{C}(\text{CH}_3)\text{C} \text{H}_2\text{CH}_3$), 1.93 (s, 3H, $\text{HN}=\text{C}(\text{C} \text{H}_3)\text{CH}_2\text{CH}_3$), 6.91 (d, 8.0 Hz, 2H, $m\text{-C}_6\text{H}_3$), 7.02 (t, 8.0 Hz, 1H, $p\text{-C}_6\text{H}_3$), 9.83 (bs, 1H, $\text{HN}=\text{C}(\text{CH}_3)\text{CH}_2\text{CH}_3$). ³¹P{¹H} NMR (23 °C, C_6D_6): δ 175.9. ¹³C{¹H} NMR (23 °C, C_6D_6): δ 9.61 ($\text{HN}=\text{C}(\text{CH}_3)\text{CH}_2\text{CH}_3$), 27.37 ($\text{HN}=\text{C}(\text{CH}_3)\text{CH}_2\text{CH}_3$), 28.91 (vt, 4.2 Hz, $\text{P-C}(\text{CH}_3)_3$), 35.06 ($\text{HN}=\text{C}(\text{CH}_3)\text{CH}_2\text{CH}_3$), 41.11 (vt, 10.8 Hz, $\text{P-C}(\text{CH}_3)_3$), 103.92, 121.64, 167.99 (C_6H_3), 179.05 ($\text{N}=\text{C}$), one [C_6H_3] signal not located. Characterization data for the *Z*-isomer (*minor*): ¹H NMR (23 °C, C_6D_6): δ 0.76 (t, 7.6 Hz, 3H, $\text{HN}=\text{C}(\text{CH}_3)\text{CH}_2\text{C} \text{H}_3$), 1.13 (s, 3H, $\text{HN}=\text{C}(\text{C} \text{H}_3)\text{CH}_2\text{CH}_3$), 1.37 (vt, 6.4 Hz, 36H, $\text{P-C}(\text{C} \text{H}_3)_3$), 2.52 (q, 7.6 Hz, 2H, $\text{HN}=\text{C}(\text{CH}_3)\text{C} \text{H}_2\text{CH}_3$), 6.90–7.00 (m, 3H, $m\text{-C}_6\text{H}_3$), 9.72 (bs, 1H, $\text{HN}=\text{C}(\text{CH}_3)\text{CH}_2\text{CH}_3$). ³¹P{¹H} NMR (23 °C, C_6D_6): δ 176.5. ¹³C{¹H} NMR (23 °C, C_6D_6): δ 10.23 ($\text{HN}=\text{C}(\text{CH}_3)\text{CH}_2\text{CH}_3$), 26.20 ($\text{HN}=\text{C}(\text{CH}_3)\text{CH}_2\text{CH}_3$), 28.95 (vt, 4.2 Hz, $\text{P-C}(\text{CH}_3)_3$), 35.12 ($\text{HN}=\text{C}(\text{CH}_3)\text{CH}_2\text{CH}_3$), 40.98 (vt, 11.0 Hz, $\text{P-C}(\text{CH}_3)_3$), 103.89, 121.70, 167.98 (C_6H_3), 179.05 ($\text{N}=\text{C}$), one [C_6H_3] signal not located.

Acknowledgment. We gratefully acknowledge funding by the National Institutes of Health (Grant No. GM 28938).

Supporting Information Available: Sample graphs for kinetic measurements and derivation of the catalytic rate expression. These data are available free of charge via the Internet at <http://pubs.acs.org>.

OM701148T